A Visual Study of Surface Potentials and Laplacians Due to Distributed Neocortical Sources: Computer Simulations and Evoked Potentials

Paul L. Nunez, Kenneth L. Pilgreen *, Andrew F. Westdorp, Samuel K. Law, and Arden V. Nelson

Summary: A "picture book" of surface potentials, Laplacians, and magnetic fields due to distributed, neocortical sources is presented. The mathematically simulated data is based on 4200 current sources at the macrocolumn scale. Estimated scalp surface maps are based on the three-concentic spheres model of the head. Emphasis is placed on the effects of sampling with a limited number of electrodes, the choice of reference electrode, and the use of the spline Laplacian to improve spatial resolution. The spline Laplacian is applied to median and ulnar nerve somatosensory evoked potentials and to auditory evoked potentials including P300. Substantial improvement in spatial resolution over conventional methods is obtained. The implementation of practical high resolution EEG systems based on the spline Laplacian is considered.

Keywords: Spline; Laplacian; Sampling; Reference electrode; SEP; P300.

The Inverse Problem

It is well-known that the "inverse problem" in EEG or MEG has no unique solution. That is, for any given potential (or magnetic field) distribution over the scalp surface, there exists a variety of possible neural current source distributions that will produce the same surface map. It should be emphasized that this is true even in the idealized case of perfect surface information. But in actual practice, surface data is recorded only at discrete locations, over only part of the surface, noise is present, models of the head are imperfect, etc. Thus, "inverse solutions" involving practical questions in EEG or MEG are typically much less unique than idealized solutions. That is, the number of possible current source distributions that may "match" (within the limits of experimental error) a given set of surface data may be quite large.

Because of the nonuniquess of the inverse problem, actual solutions involve the "constrained inverse problem", in which information about neurophysiology and anatomy is used to limit possible source distributions. The three most common constraints are:

1. The sources consist of a single or small number of "dipoles", typically at linear scales of about 1 cm or larger. The word "dipole" is used to indicate the "current polarization", or dipole moment per unit volume in this context. For precise definition, refer to Nunez 1989a,b, 1990b; Nunez et al. 1991. This subfield of the inverse problem, called "dipole localization", has been developed in both EEG (Henderson et al. 1975; Kavanaugh et al. 1978; Nunez 1981; Fender 1987; Cuffin et al. 1991) and MEG (Cuffin and Cohen 1979; Hari and Kaukoranta 1985; Weinberg et al. 1987; Williamson and Kaufman 1987; Romani and Rossini 1988; Cohen et al. 1990).

2. Sources, e.g., dipoles, may change strength, but not location or orientation over some specified time interval. This "spatial-temporal" constraint has recently been added to dipole localization algorithms (Scherg and von Cramon 1985, 1989; Scherg 1989). Also, refer to review by Nunez (1990b).

3. Sources are all located at the same depth, e.g., in neocortex. This subfield of the inverse problem in EEG has been labeled, "spatial deconvolution" (Nicholas and Deloche 1976), "software lens" (Freeman 1980), "de-blurring" (Gevins 1989), or "cortical imaging" (Kearfott et al. 1991). It is based on the unique relationship between surface potentials and sources at a fixed depth (Katznelson 1981; Nunez 1987b).

Brain Physics Group, Department of Biomedical Engineering, Tulane University School of Engineering, New Orleans, Louisiana
*Also with Alabama Neurophysics Laboratory Anniston, Alabama
Accepted for publication: July 2, 1991.
The authors greatfully acknowledge the technical assistance of Chris Fritton, Laurie Orth, and Chiraprakash Nayak. This research was supported by NIH grant RO1 NS24314.
Invited paper, Submitted to Brain Topography, July, 1991
Correspondence and reprint requests should be addressed to Dr. Paul Nunez, Department of Biomedical Engineering, Tulane University School of Engineering, New Orleans, Louisiana, 70118.

A major issue in EEG or MEG concerns the appropriateness of these constraints in specific applications. For example, a single dipole may be assumed to be the source of a visual evoked potential due to half visual field stimulation, and the dipole then located at the correct location in the contralateral hemisphere (Wood 1982). In studies of patients with known, implanted dipole sources, localization accuracy with either EEG or MEG is typically of the order of 1 cm (Cohen et al. 1990; Cuffin et al. 1991). While this approach has a number of apparent applications (e.g., location of epileptic foci), we call into question its general extension by others to cases of unknown sources which may be distributed over large regions of the brain. Of course, when confronted, dipole localizers of distributed sources, may emphasize that these are only "equivalent dipoles", a purely descriptive concept used to help quantify the observed spatial distribution of potential or magnetic field. However, there are many other (and we believe, much better) ways to quantify EEG/MEG data, which do far less violence to realistic views of neurophysiology and neuroanatomy.

Surface Laplacians of EEG

Partly because of the arguments expressed above, we have emphasized the surface Laplacian (also called, "current source density", or "radial current estimate") in the study of unknown sources of EEG. Estimation of the surface Laplacian is mostly independent of volume conductive models of the head, and does not represent a solution to the inverse problem. However, it acts as a spatial filter which emphasizes local sources (both tangentially and in depth) over distant sources (Hjorth 1975; Nunez 1981, 1988, 1990b; Perrin et al., 1987a,b; Nunez et al. 1991, Nunez and Pilgreen 1991; Law 1991). The physical interpretation of the surface Laplacian is that it provides an estimate of local skull current flow from the brain into the scalp. The fact that it has a real physical basis, rather than just some ad hoc mathematical transformation, partly explains its success. When applied to either mathematically simulated data (i.e., known sources in layered spheres models of the head) or actual EEG data (provided the spacing between electrodes is less than about 3 or 4 cm), it provides dramatic improvement in spatial resolution.

In the case of localized cortical sources, the surface Laplacian can be used to find equivalent dipoles. However, the surface Laplacian estimate also works quite well for distributed cortical sources. The Laplacian estimate is not sensitive to deep sources. In this sense, it is similar to spatial deconvolution, and the two methods may be naturally applied simultaneously to the same data set to provide a check for consistency (Gevins 1987).

The Forward Problem

The "forward problem" in EEG or MEG is concerned with the calculation of surface potentials or magnetic fields due to known source distributions. The accuracy of these calculations depends on the accuracy of the volume conductive model of the head. The most useful EEG model for most purposes consists of three or four concentric spherical surfaces, representing brain, CSF (4--sphere only), skull and scalp (Rush and Driscoll 1968, 1969; Kavanagh et al. 1978; Cuffin and Cohen 1979; Nunez 1981; Fender 1987). While more accurate geometric models have been applied (Sepulveda et al. 1983; Cuffin 1985; He et al. 1987; Yan et al. 1991; Gevins et al. 1991), such numerical methods are limited in accuracy by knowledge of boundaries and resistivities of various tissues. Furthermore, layered-sphere models are much easier to apply and far less computationally intensive. The later issue is especially important for cases, like those presented here, in which a large number of simulations of distributed source effects is carried out.

In several of the following sections, we use forward solutions to demonstrate the likely effects of various experimental conditions on surface estimates of potential, Laplacian, and magnetic field. We suggest that this visual study of the forward problem may help the investigator both in the design of better experiments and in the physiological interpretation of surface data. In later sections, application of some of these ideas to evoked potential phenomena is presented.

The pictorial tool of this study is NCAR (National Center for Atmospheric Research) Graphics, originally developed to map isocontours of temperature, pressure, etc. on the surface of the earth. The upper hemisphere of the "earth" (cortex) is divided into 4200 elemental surfaces, representing macrocolumns of area $\Delta A \sim 0.1$ cm^2. Each macrocolumn produces a radial "dipole" (e.g., polarization at this scale) expressed in terms of the potential difference $\Delta\phi$ across each small surface ΔA. The relationships between $\Delta\phi$ and other physical variables, e.g., dipole moment, are shown in (Nunez 1981, 1989b, 1990b). In addition, one simulation includes tangential dipoles, representing sources in fissures and sulci.

Source magnitudes are here expressed in terms of transcortical potential differences $\Delta\phi$ rather than dipole moments because the former are measured directly with "micro-EEG" electrodes (Lopes da Silva and Storm van Leeuwen 1973; Petsche et al., 1984, review by Nunez 1981, 1990b). Thus, we can obtain realistic estimates of the actual magnitudes of surface potential for various source distributions in the surface maps. In our simulations, source magnitudes vary between $\Delta\phi$ = -200 to +200 μV. An example is shown in figure 1, in which the maximum scalp potential increases from the 4 μV range to the 18 μV

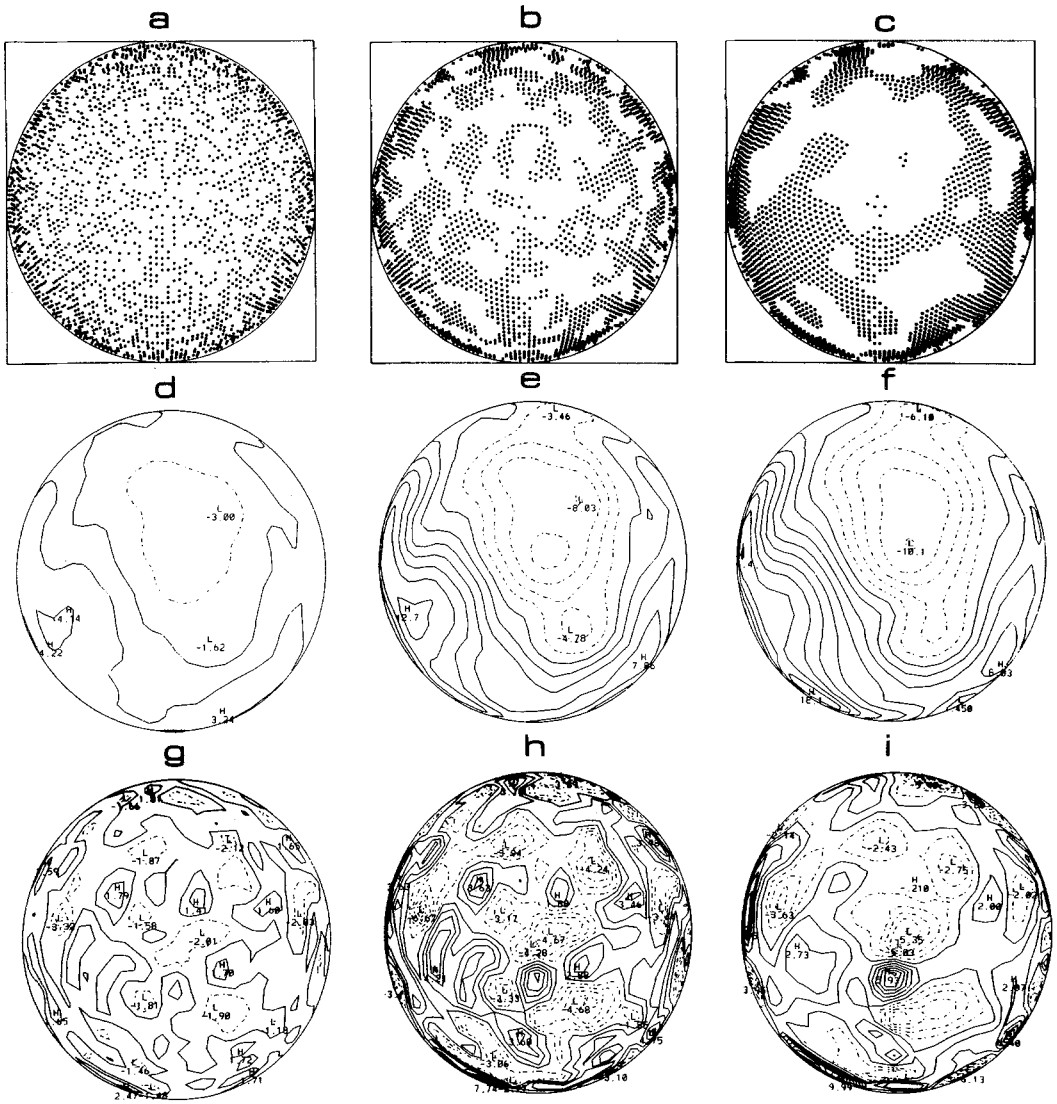

Figure 1. Upper row. Simulation of cortical sources at the macrocolumn scale. Each of 4200 locations (e.g., macrocolumns) on the upper hemisphere contributes a source $\Delta\phi$ equal to the potential difference across the macrocolumn, where $\Delta\phi$ is proportional to effective dipole moment. Positive sources are indicated by dots, negative sources by blank spaces. In the far left plot, sources vary randomly between -200 and +200 μV. "Clumping" is simulated by an iterative process in which sources are determined partly by eight nearest-neighbor sources and partly by random input. The middle and left-most plots are obtained after three and nine iterations, respectively. The nose is assumed to be at the top of all plots (for later reference). Middle row. Scalp surface potential (with respect to infinity). Maps are simulated using a three-concentric spheres model of the head with a brain to skull resistivity ratio of 80. Each of the 4200 sources contributes to the surface potential at 648 locations. Isopotential lines (expressed in μV) are drawn through each of these points without interpolation, using the NCAR software package. Solid lines are positive or zero; dashed lines are negative. Local minima and maxima are indicated by L and H, respectively. Crowding at the edges is due to the perspective of an observer looking down on the top of the head. Edge detail can be obtained by map rotation if desired. Lower row. Laplacian maps are shown. Isocontours are expressed in $\mu V/cm^2$. By contrast to the potential plots, all large scale source features (especially those in the third column) are revealed by the Laplacian maps.

range as the effective correlation length of the dipole layer of macrocolumn sources is increased, i.e., as the source distribution becomes more "clumped". It should be noted that this important relationship between effective correlation length (or coherency in the case of dynamic patterns) and scalp amplitude is supported by a number of experiments involving the simultaneous recording of cortical and scalp potentials (Cooper et al. 1965; DeLucchi et al. 1975; Nunez 1981; Katznelson 1982).

The potential, Laplacian, or radial magnetic field component at each scalp surface location is due to the summed contribution from each of the 4200 dipole sour-

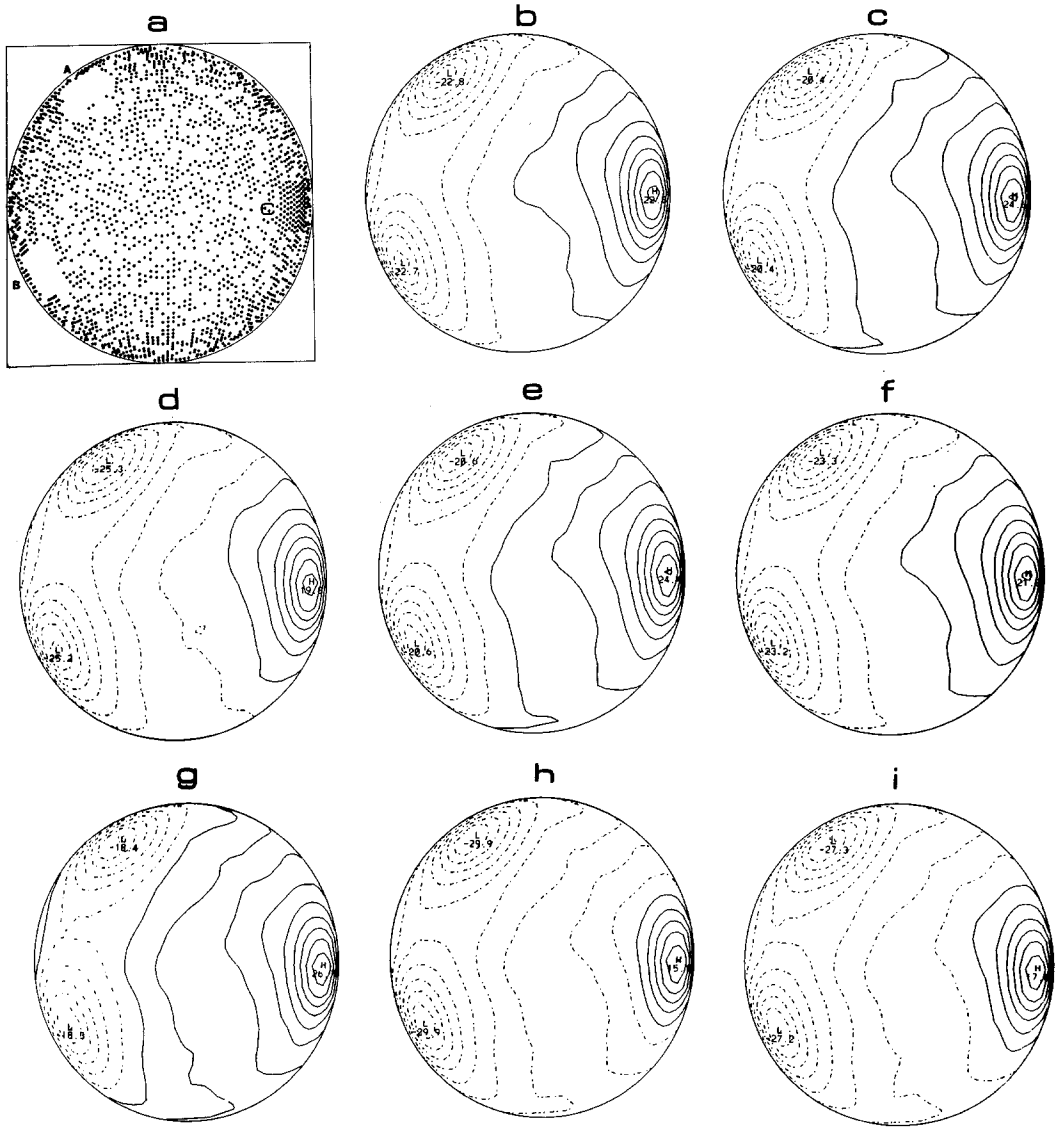

Figure 2. **a**. An example source distribution with two negative (A and B) and one positive clumps (C). Random sources vary uniformally between -200 and +200 μV; clump sources are either + or - 200 μV. **b.** Potential with respect to infinity (μV), simulated in the manner of figure 1. **c**. Average reference potential. **d**. Linked-ears reference potential with balanced ear contact resistances (R1 = R2), assumed large enough to prevent a shorting effect. **e**. Left ear (A1) reference potential. **f**. Unbalanced left (R1/R2 = 2/5), linked-ears potential. **g**. Nose reference potential. **h**. Right ear (A2) reference potential. **i**. Unbalanced right (R1/R2 = 5/2), linked-ears potential. Refer to Table 1.

ces, as calculated using the three-concentric sphere model. In some simulations, surface estimates of potential, etc., are obtained at 648 scalp locations and isocontours plotted with no interpolation. Surface estimates are also obtained at fewer locations (31, 48, 117) and submitted to nearest-neighbor or spline interpolation in order to simulate the effects of discrete sampling with EEG electrodes. Potentials are calculated with respect to various references. Laplacians are also estimated using the spline methods with various numbers of simulated electrodes.

The Reference Electrode

The issue of the reference electrode continues to be raised in EEG and evoked potential studies. A particular reference choice may be regarded as a spatial filter which emphasizes certain sources at the expense of others (Nunez 1988). This feature partly explains why there has been no final resolution of this issue in EEG. The effects of various references on surface potentials due to a particular pattern of distributed sources are illustrated in figure 2. Since the surface is sampled at 648 locations and no interpolation is applied, the contours have nearly

Table 1. Amplitude ratios of potentials calculated at C3/C4 and T3/T4 as a function of reference for the source distribution of figure 2a.

	Reference	Reference potential (μV)	Amplitude C3/C4	Amplitude T3/T4
b	∞	0.0	-1.4	-0.3
c	average	-2.3	-0.7	-0.1
d	R1 = R2	+2.5	-3.3	-0.5
e	A1	-2.1	-0.7	-0.1
f	R1/R2=2/5	+0.5	-1.6	-0.3
g	Nose	-4.4	-0.3	-0.0
h	A2	+7.2	+10.3	-1.0
i	R1/R2=5/2	+4.5	-10.4	-0.7

identical shapes, with differences mainly due to the addition of constant potentials to each surface location. Other slight differences occur because contours are plotted at fixed levels (3, 6, 9, etc. μV) in each map so that contours pass through somewhat different locations with different references. Of course, *actual* isopotential lines as opposed to *plotted* lines have identical shapes, independent of reference electrode (with possible exception of the linked-ears reference).

The linked-ears (or mastoids) reference may, in some applications, lead to one or both of the following problems (Katznelson 1981; Nunez 1988, 1990a):

1. If contact resistances (e.g., "electrode resistances") at the ears are too small, there may be a significant shorting effect which acts to reduce asymmetry of measured scalp potentials over that which occurs naturally. While this effect may be negligible in most applications, its magnitude depends on source location, volume conduction (including various holes in the skull near the ears), and ear contact resistances (which are never stated in publications); therefore, it is a difficult effect to estimate accurately.

2. If ear contact resistances are not equal, the effective reference is unbalanced towards one or the other ear, e.g., if the contact resistance at the left ear is much larger than that of the right ear, the effective reference is the right ear.

Mathematical simulation of problem (1) cannot be obtained with the usual layered-sphere models since the wire connecting the ears alters natural boundary conditions. Hence, this effect is ignored here. However, problem (2) is illustrated in figure 2, in which cortical sources are randomly distributed except for two negative (A,B) and one positive (C) "clumps". Because of cancellation of positive and negative contributions in the random dipole layer, the surface potential with respect to ∞ (b) indicates only the contributions from the "clumps" (e.g., small correlated dipole layers). In plot (f), left and right ear contact resistances are assumed to be 2kΩ and 5kΩ, respectively. The resulting contour map is similar to plot (e) for the A1 reference. When the linked-ear reference is unbalanced the other way (i), the resulting contours are similar to those of the A2 reference (h). The contour shapes plotted in figure 2 are nearly identical for all references, as expected.

Suppose we imagine a simple experiment (similar to a number of published EEG or EP experiments) in which ratios of amptitudes of potential at several homologous electrode sites are obtained as a function of clinical or cognitive state. We further imagine that when placing electrodes, the technician faithfully follows standard procedures, e.g., electrode contact resistances are all below 5kΩ, but no attempt is made to balance ear electrode resistances.

Amplitude ratios (C3/C4 and T3/T4) for the source distribution of figure 2 are listed in Table 1 for various choices of reference. Also, the potential at the reference (with respect to ∞) is listed. Here R1 and R2 refer to contact resistances at the left and right ears, respectively. The case R1=R2 is the balanced, linked-ears reference which is identical to mathematically linked ears. As expected, amplitude ratios can be almost anything; they are highly dependent on reference. Certainly, no project involving a pool of subjects is likely to deliberately mix data using different references. However, use of the unbalanced linked-ear reference is, in practice, equivalent to changing references. That is, as this procedure is apparently carried out in some (if not most) laboratories, it is essentially a "random reference" approach, which may confound statistical measures in a pool of subjects. We do not claim that published qualitative conclusions regarding correlation between clinical or cognitive state and EEG are automatically wrong if based on linked-ears data. Rather, we suggest that this is a poor choice for many kinds of studies, which may significantly contaminate quantitative correlations, especially since the physically linked-ears reference is easily replaced (by mathematically linked ears, for example). It is quite possible that some lateralization measures may be more robust than suggested by published data when obtained with a more appropriate reference or better still, a Laplacian measure (Nunez 1981; Katznelson 1981; Nunez 1990b; Nunez and Pilgreen 1991).

What is the best choice of reference? From row f, column 2 of Table 1, note that the "unbalanced-left,

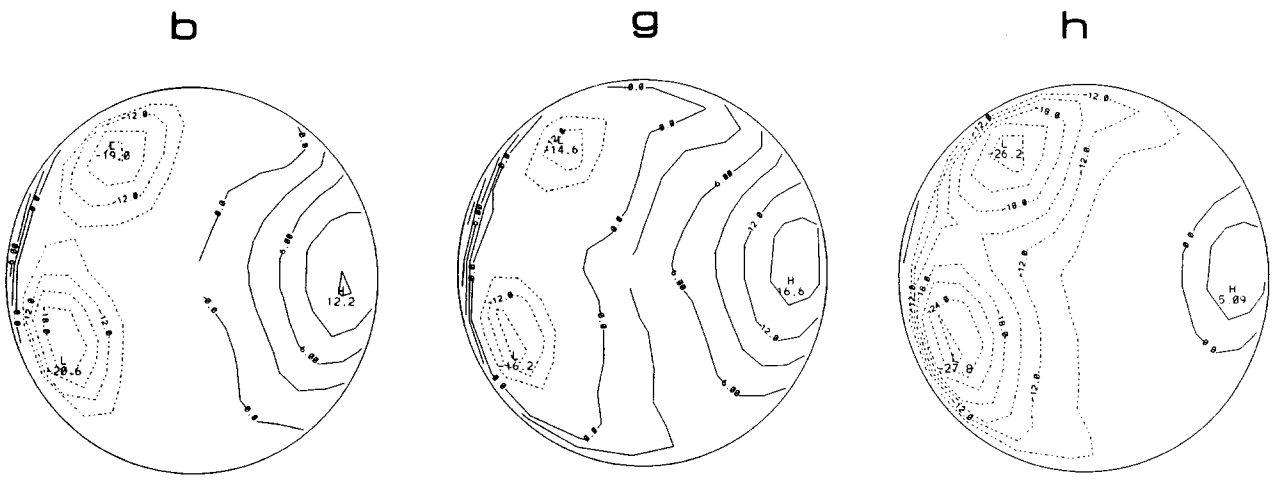

Figure 3. Potential maps for source distribution and references identical to b,g, and h of figure 2, except potentials have been sampled only at the 31 electrode positions shown in a. These 31 potentials were submitted to a 3-dimensional spline interpolation, resulting in surface potential estimates at 144 locations. Isopotential lines are then drawn through these locations without further interpolation.

linked-ears reference" is "best" for the source distribution of figure 2 since it provides the reference potential closest to zero of those considered. Of course, this is just a coincidence. With other source distributions, any other reference choice might be "best" in this sense. For example, had we chosen equal number of positive and negative clumps of equal size, the average reference potential would have been close to zero. Or, if all clumps were close to the left ear, the right ear might provide the "best" reference. Of course, in the study of brain dynamics, e.g., following the changing source distribution of an evoked potential as a function of latency from the stimulus, the "best" reference can also be expected to change with latency.

Consider the implications of the above arguments for evoked potential studies. The latencies of peaks in evoked potentials must be partly reference-dependent (Nunez 1990a). This can be partly appreciated by noting that at any fixed latency, there is always some choice of reference that will yield zero potential at a particular "recording" electrode, i.e., no peak can occur at this latency. The change of waveform of the somatosensory evoked potential obtained with an average reference, rather than the ear reference ipsilateral to the stimulus side, has been emphasized (Desmedt and Tomberg 1990; Desmedt et al. 1990). While these studies correctly point to the apparent advantages of using a "distant" reference electrode when studying *known*, localized sources, it must be emphasized that such arguments fail when applied to *unknown* sources. For example, if one wished to map both the contralateral and ipsilateral somatosensory evoked response as a function of latency, the ipsilateral ear would be a poor choice of reference, if for no other reason than its asymmetric location. We might reasonably choose a frontal reference in this case. But, a frontal reference is no good if we are interested in possible late frontal sources of the SEP. If our goal in mapping evoked potentials is to obtain information about the location of unknown "clumps of sources" (i.e., regions of correlated sources), reference-free methods (e.g., the Laplacian) would seem more appropriate.

It should also be noted that the question of "best" reference may have little to do with whether the reference is "active" in the sense of nearby sources; all references in our examples have close, active sources. Furthermore, inhomogeneities (e.g., skull holes) effectively produce "secondary" (e.g., fictitious) sources which contribute to reference potentials (Nunez 1981, 1988). These arguements are, of course, just a reflection of the fact that scalp potentials generally depend on the location of *pairs* of electrodes so that the usual distinction made in EEG studies between "recording electrode" and "reference electrode" is largely fictitious (Rush and Driscoll 1969; Nunez 1981, 1988, 1990a; Katznelson 1981).

In figure 3, three of the potential contours of figure 2 are re-plotted using standard 10/20 sampling (31 locations) with a 3D spline interpolation (Law 1991), which is an extension of the smooth, 2D spline originally developed to describe the surface of an airplane wing and later applied to EEG (Perrin et al. 1987a). In figure 4, we show the same simulated data as standard Pathfinder maps, which use nearest-neighbor (triangular) interpolation. Since we have chosen a simple, large scale clump distribution, all potential maps yield, in this case, a reasonably accurate idea of the underlying clumped (correlated) sources.

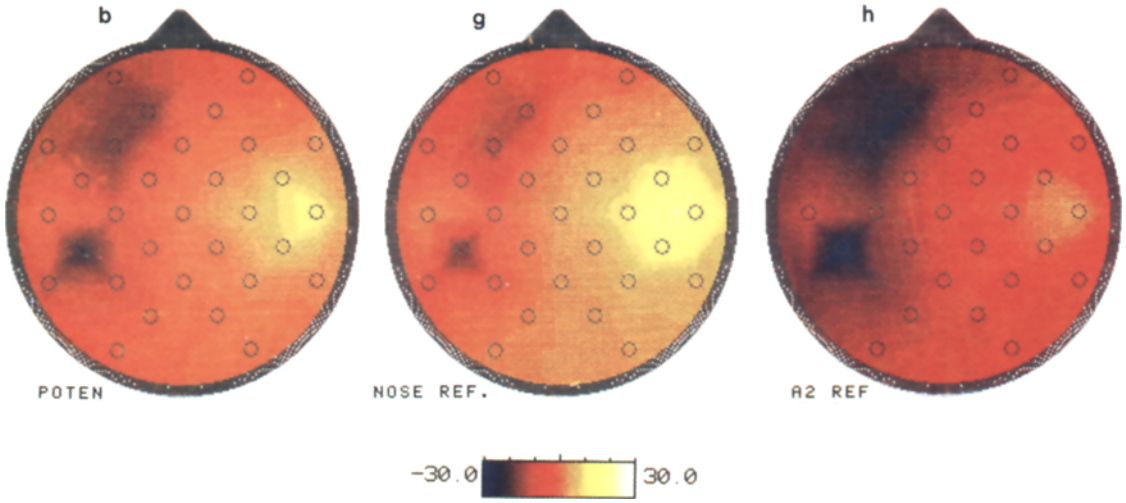

Figure 4. Same simulated data shown in figure 3 except that potentials at the 31 locations have been submitted to Pathfinder for color plotting using nearest-neighbor (triangular interpolation). Note that accuracy is inferior to equivalent plots shown in figure 3.

In figure 5, we have choosen more complex pattern of sources. The potential and Laplacian maps are again constructed using 648 surface samples. We note that the potential map (b) yields a misleading picture of the source distribution. That is, it does indicate the negative clump at E and the major positive clump just below and to the left of E. However, it misses most of the other detail, showing, for example, all negative potentials over the far left region, even though this region contains several positive clumps. Furthermore, the potential map shown here is the idealized potential with respect to infinity. Reference electrode effects may further confound its interpretation. By contrast, the Laplacian map (c) shows nearly all of the major features, including major "canyons" (A-H) and peaks. It is also independent of reference.

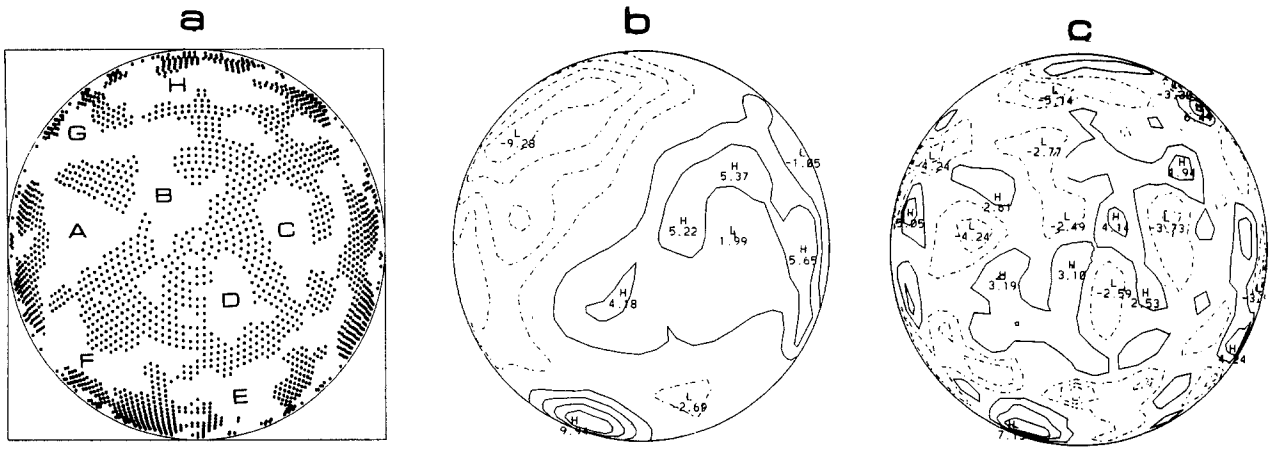

Figure 5. **a**. An example source distribution exhibiting more complexity than the three clumps of figure's 2-4. Major regions of negative sources are indicated by letters A-H. **b**. Isopotential lines (μV, with respect to infinity) fail to pick out much of the detail of the source distribution. For example, the region roughly bordered by FBHGA is composed of a mixture of positive and negative sources, but potentials over this region are all negative. Isopotential lines do, however, correctly locate the major positive clump just below and to the left of E. In practice, potential estimates are further confounded by reference electrode effects and interpolation-induced errors. **c**. The corresponding surface Laplacian ($\mu V/cm^2$). All major details of the sources are revealed, including major "canyons" (A-H) and peaks, e.g., at bottom, on both sides, and just below and above A and C.

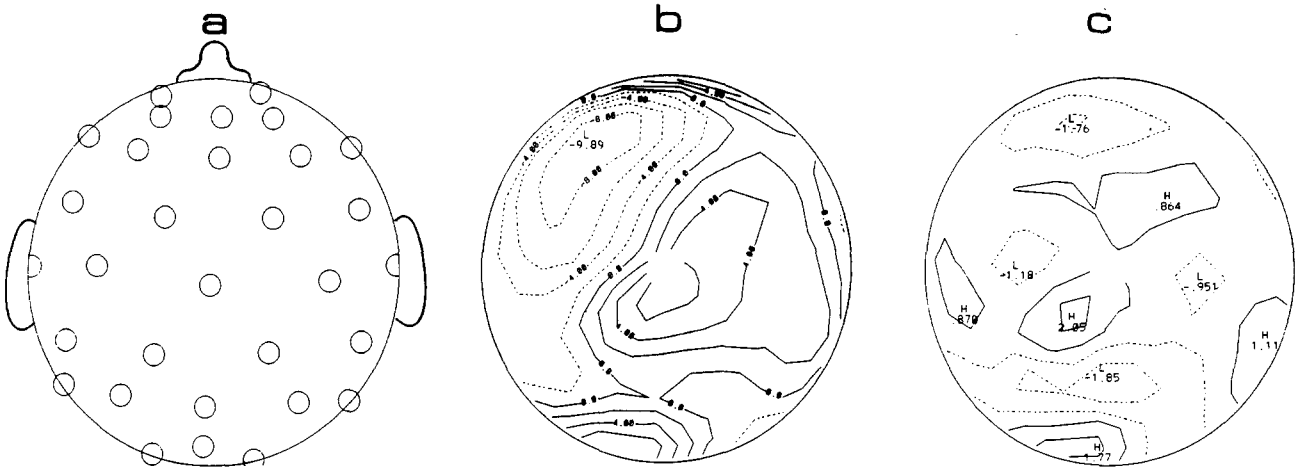

Figure 6. **a**. Simulated electrode locations (31) used to estimate potentials and Laplacians due to sources shown in figure 5a. **b**. Potential map equivalent to figure 5b, based on 3-dimensional spline interpolation and 31 sampled locations. **c**. Spline-Laplacian equivalent to figure 5c.

The plots of figure 5 are, of course, based on an unrealistically high sampling density. Thus, in figures 6-8 we show the effects of various sampling density with the same source distribution. That is, the potential in figure 5b is sampled at 31, 48, and 117 locations, as shown by the equivalent electrode positions in Fig's 6a, 7a, and 8a, respectively. These sets of potentials were submitted to 3-dimensional spline interpolation and Laplacian estimation. The improvement in spatial resolution which parallels increased electrode density is much more evident for the Laplacian maps than for the potential maps.

For comparitive purposes, we show Pathfinder T-maps of potential based on the same 31 and 48 locations for the sources of figure 5a, in figure 9. The mapping protocol is limited to 48 interpolation points and restricted to nearest-neighbor interpolation so we are not able to provide a full comparison to Fig's 6-8. These results call attention to an important paradox in surface mapping as currently produced with most commercial systems: the inverse relationship between the "beauty" of color maps and the accuracy possible with flexible, black and white plotting packages. Of course, it is quite posible to have both color and accuracy, but, thus far, most commercial systems have opted only for the former feature.

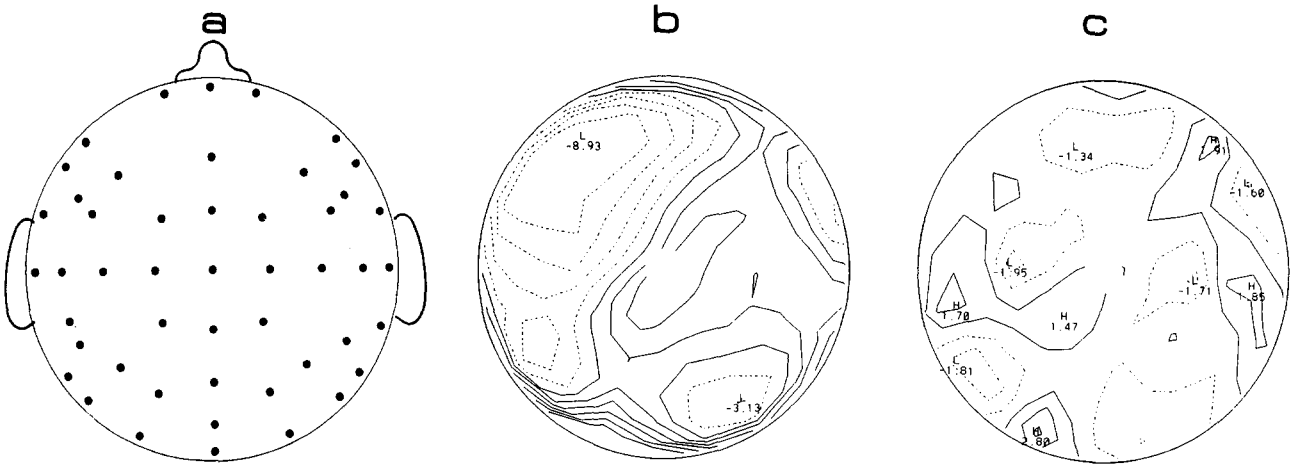

Figure 7. **a**. Simulated electrode locations (48) for source distribution in figure 5a. Electrode representation is reduced in size to prevent overlap at the edges. **b**. Spline potential equivalent to figure 5b. **c**. Spline Laplacian equivalent to figure 5c.

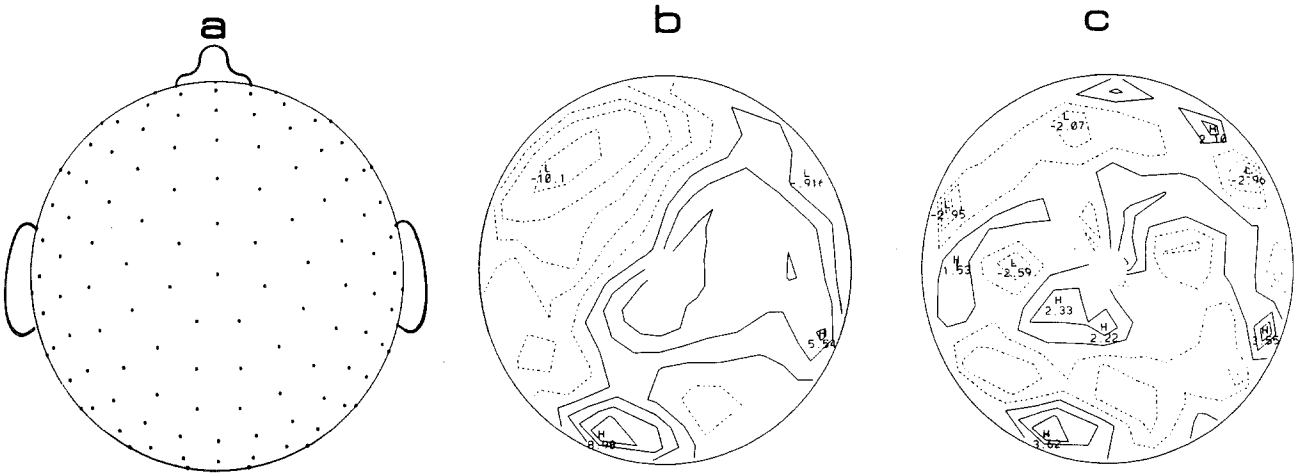

Figure 8. **a**. Simulated electrode locations (117) for source distribution in figure 5a. **b**. Spline potential equivalent to figure 5b. **c**. Spline Laplacian equivalent to figure 5c. Note that both the spline based potential and Laplacian converge to the "correct" patterns shown in figure 5. However, only the Laplacian yields an accurate picture of the source pattern.

Magnetic Fields

We have illustrated that EEG electrodes are selectively sensitive to subsets of brain sources. Cortical sources in gyri are closer to the surface and, for this reason alone, tend to produce larger scalp potentials than midbrain sources or sources in fissures and sulci. Furthermore, tangential cortical dipoles tend to produce smaller scalp potentials than radial dipoles due to partial cancellation of positive and negative contributions (Cuffin and Cohen 1979). Finally, even the category of radial dipoles in gyri may be further subdivided into random and correlated dipole layers. Only the latter typically produce scalp potentials of sufficient magnitude to be recorded on the scalp without averaging (Nunez 1981; Katznelson 1982), as illustrated in figure 1.

The magnetoenephalogram (MEG) provides an estimate of the local component of the magnetic field vector perpendicular to the scalp. This measure of brain activity is of interest mainly due to its lack of distortion when passing through the skull. Thus, much of the field spreading of potentials by volume conduction is avoided. While the MEG, like the EEG, is produced by neural current sources, it is apparently sensitive to a much smaller subset of sources than is the EEG. This occurs mostly because the radial magnetic field component due to a radially

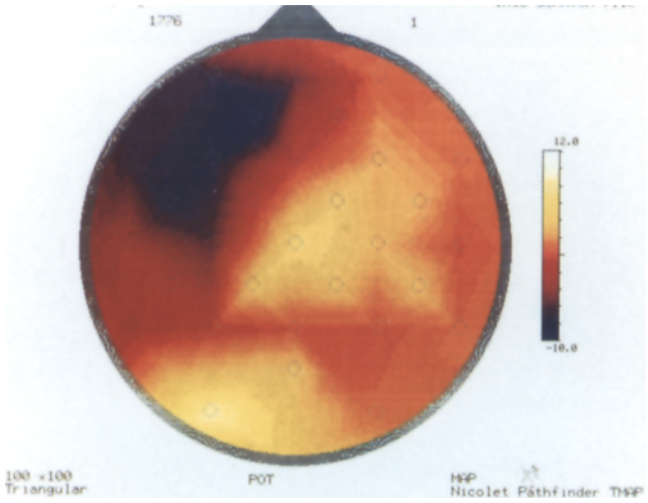

Figure 9. **a**. Pathfinder T-map potential for sources of figure 5a constructed with triangular interpolation and 31 sampled points, equivalent to figure 6b.

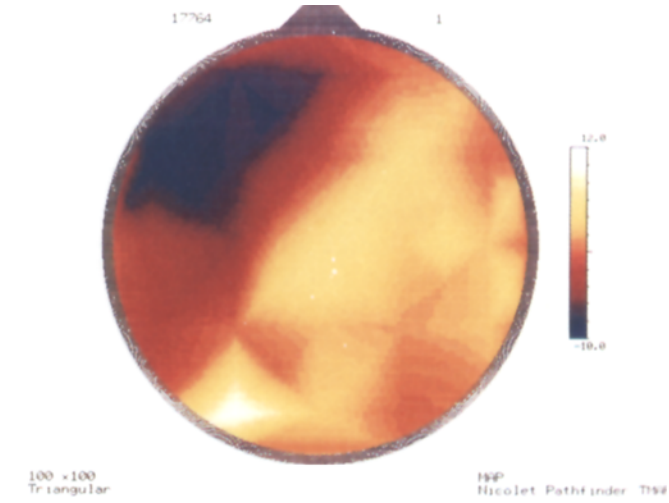

Figure 9. **b**. T-map based on 48 sampled points, equivalent to figure 7b. Note that increased spatial resolution due to additional channels is limited by interpolation accuracy.

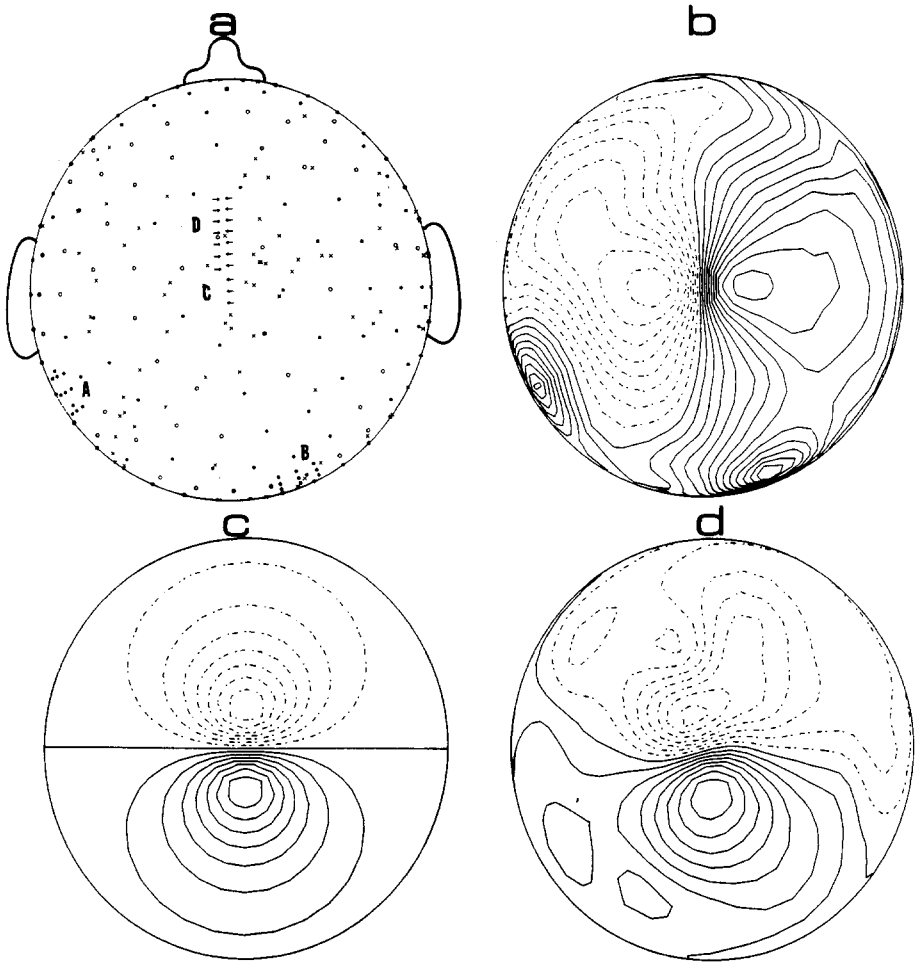

Figure 10. **a**. Assumed source distribution consisting of positive radial dipoles (dots), negative radial dipoles (open circles), directed tangential dipoles of fixed magnitude (arrows), and random (in both magnitude and direction) tangential dipoles (crosses). Source strenghts of tangential dipoles are made five times larger than those of radial dipoles to simulate adjacent dipoles at varous depths of fissures and sulci. **b**. Surface potential map based on 648 surface samples with no interpolation. Solid lines indicate positive potentials with respect to infinity. The two positive clumps of radial dipoles (A and B) and unapposed dipole layer (C) make the major contributions to the potential map, with much less contribution from either random or apposed dipoles (D). **c**. Map of radial component of magnetic field (MEG) due only to the unapposed dipole layer (C), obtained from equations given in (Nunez 1986). **d**. The MEG map due to all sources (similar to map c).

oriented dipole in a spherically symmetric volume conductor is zero (Cohen and Cuffin 1979; Williamson and Kaufmann 1987; Romani and Rossini 1988). Thus, by implication, dipoles in cortical gyri make small contributions to MEG. Furthermore, opposing dipoles in fissures and sulci tend to produce cancelling magnetic fields as in the case of EEG. Thus, the MEG produced by a correlated dipole layer can be expected to be largest at edges of the layer where regions of noncancelling tangential dipoles occur (Nunez, 1986, 1989a, 1990b).

In order to illustrate these ideas, we have presented a simulation of MEG and potential maps due to a collection of radial and tangential dipoles in figure 10. The selective sensitivity of the MEG to the alligned and unopposed tangential dipoles at the center of the surface (C) is evident. The implications of these and other studies of EEG (Cohen and Cuffin 1979; Nunez 1981; Cohen et al. 1990; Cuffin et al. 1991) and MEG (Cohen and Cuffin 1979; Nunez 1986; Wikswo and Roth 1988; Cohen et al. 1990) are as follows:

1. If a particular phenomena is due to a localized "source" (more accurately pictured as a localized "clump" of correlated dipoles at small, e.g., macrocolumn scales), either EEG and MEG is apparently able to localize such sources with typical accuracy of about 1 cm. Cortical sources in

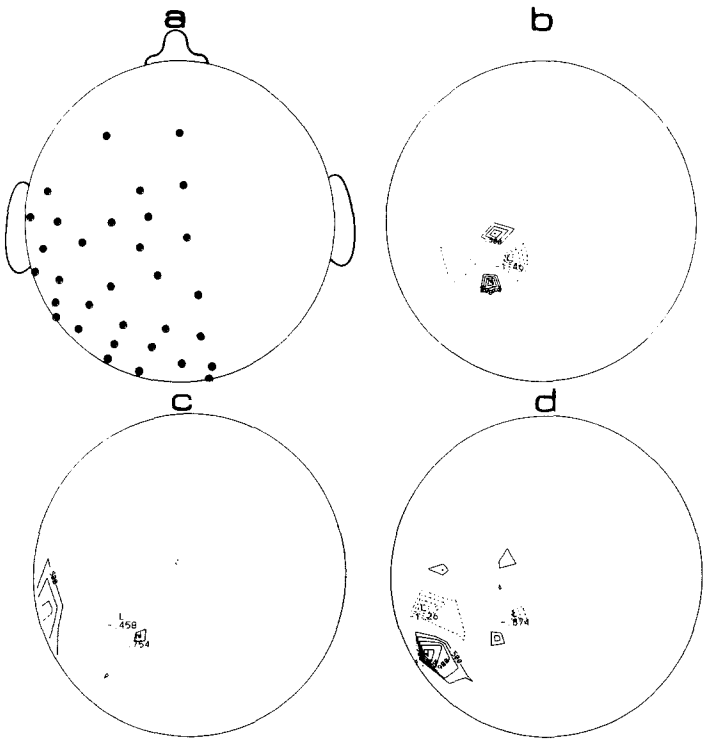

Figure 11. **a.** Electrode locations (32) over contralateral hemisphere used for SEP studies. Note that coverage of the space is more dense than indicated since electrodes are much larger than the dots shown. **b.** P9 (i.e., 9 ms latency) Laplacian map. "Background Laplacians" have been subtracted from each map so that pre-stimulus map is blank. **c.** N15 Laplacian map. **d.** P20 Laplacian map (Law 1991).

gyri are better localized by EEG; ideally, sources in fissures and sulci are better localized by MEG.

2. When sources are distributed, the MEG and, to a lesser extent, the EEG may provide a false localization. That is, these methods may correctly localize the particular subset of sources to which they are most sensitive and ignore all other sources. This procedure may then yield a very unrealistic picture of the underlying physiology, if not properly interpreted. Possible examples are "localization" of interictal spikes with multiple, nonstationary foci and "localization" of the sources of alpha rhythm.

Somatosensory Evoked Potenitals

In order to test the surface Laplacian on real physiological data, we have first chosen a widely studied phenomena for which cortical sources are apparently well-localized, the somatosensory evoked potential (SEP) (Regan 1989). At the time of this writing, data on three subjects have been fully analyzed. Details of the experimental protocol are presented in (Law 1991); a short outline follows:

1. A commercial cap with 117 electrode locations having near uniform spacing was place on the head. A 32-electrode subset over the left hemisphere was chosen for the somatosensory studies as shown in figure 11. Average electrode spacing was about 2 cm.

2. A simple bite bar was used to stabilize the head. A commercial 3-dimensional digitizer (connected to a PC) was used to digitize the head surface under the chosen electrode array.

3. A nonlinear regression routine (Statistical Analysis Software - SAS) was run on the campus mainframe IBM 3081 GX in order to fit the surface to the best fit sphere (Law and Nunez 1991).

4. Scalp potentials were recorded with a Pathfinder I equipped with 32 input channels. Filters on the Pathfinder were set at 5 and 3000 Hz. The mid-point between the nasion and Fpz was used as the reference electrode location. Both median and ulnar nerve stimulation were applied two cms proximal to the wrist, with stimulating cathode distal to the anode. The threshold level of stimulation was defined when the thenar muscle elicited a muscle twitch for median nerve stimulation. Ulnar nerve threshold was defined when a muscle twitch is

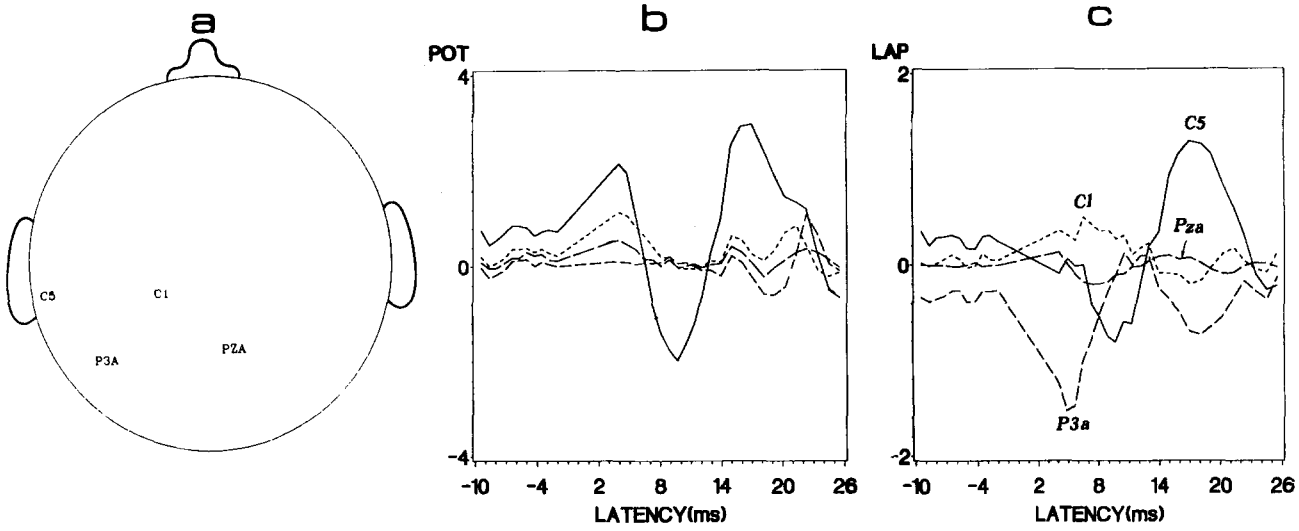

Figure 12. Potential (middle) and Laplacian (right) time series for four (of 32) data channels shown at left, obtained for median SEP stimulation. Grand average of three trials for subject MV (Law 1991).

elicited in the little finger. This same current level was used for stimulation. Evoked potentials were obtained with averages based on 500 to 700 stimuli. Records were obtained for a period ranging between 10 msec pre-stimulus to 30 msec post-stimulus. No special filtering or artifact removal was applied to increase the signal to noise ratio. Three trials were carried out on subject MV (discussed here) for each nerve stimulated.

5. Averaged scalp potentials were transferred to the campus mainframe computer in order to fit the potential data to a spline using a new 3-dimensional interpolation approach (Law 1991) and subsequent calculation of the surface Laplacian map based on the best-fit spherical surface (Perrin et al. 1987 a,b, 1989; Nunez 1989c, 1990b; Nunez and Pilgreen 1991; Law 1991). Laplacian estimates at 144 locations within the elctrode array were obtained.

6. The Laplacian data was then transferred to the departmental VAX 3600 minicomputer for plotting of Laplacian isocontours (with no further interpolation) using standard NCAR software, the same package used to map potentials and Laplacians due to the mathematically simulated sources discussed in earlier sections.

The potential and Laplacian waveforms for four channels (grand average of 3 trials) are shown in figure 12 for the case of median nerve stimulation. Laplacian maps corresponding to four time slices are shown in figure 11. A "background Laplacian" was defined as the maximum Laplacian value obtained at all 144 surface locations and 6 pre-stimulus times (a total of 6 x 144 = 864 Laplacians) so that the pre-stimulus map is, by definition, blank. We have chosen this conservative plotting strategy to insure that the contours presented here represent actual cortical sources time-locked to the stimulus. In so doing, we may have eliminated other sources which are "really there." The issue of appropriate background level for the Laplacian requires further study.

The trial-to-trial consistency of evoked potentials and differences between Laplacian maps generated by median and ulnar nerve stimulation are illustrated in figure 13. There is no significant difference between maps obtained in the three trials. However, the spatial patterns corresponding to different nerves are quite distinct, thereby illustrating the apparent utility of the surface Laplacian in revealing subtle but robust differences in evoked Laplacian maps. While the cortical sources of the SEP's are approximately in the correct anatomical locations, we cannot be more precise about accuracy without MRI data, which is not yet available on these subjects. Other subjects showed significantly different Laplacian patterns, although all exhibited trial- to-trial consistency, and all major sources were in approximately the correct anatomical location near the somatosensory cortex.

The Auditory P300

In order to test the spline-Laplacian on a phenomenon whose sources are not well-understood, we have obtained auditory evoked potentials using the standard odd-ball paradigm (Regan 1989). At the time of this writing, four subjects have had their data analyzed. A report on one subject (KP) with data recorded in a different

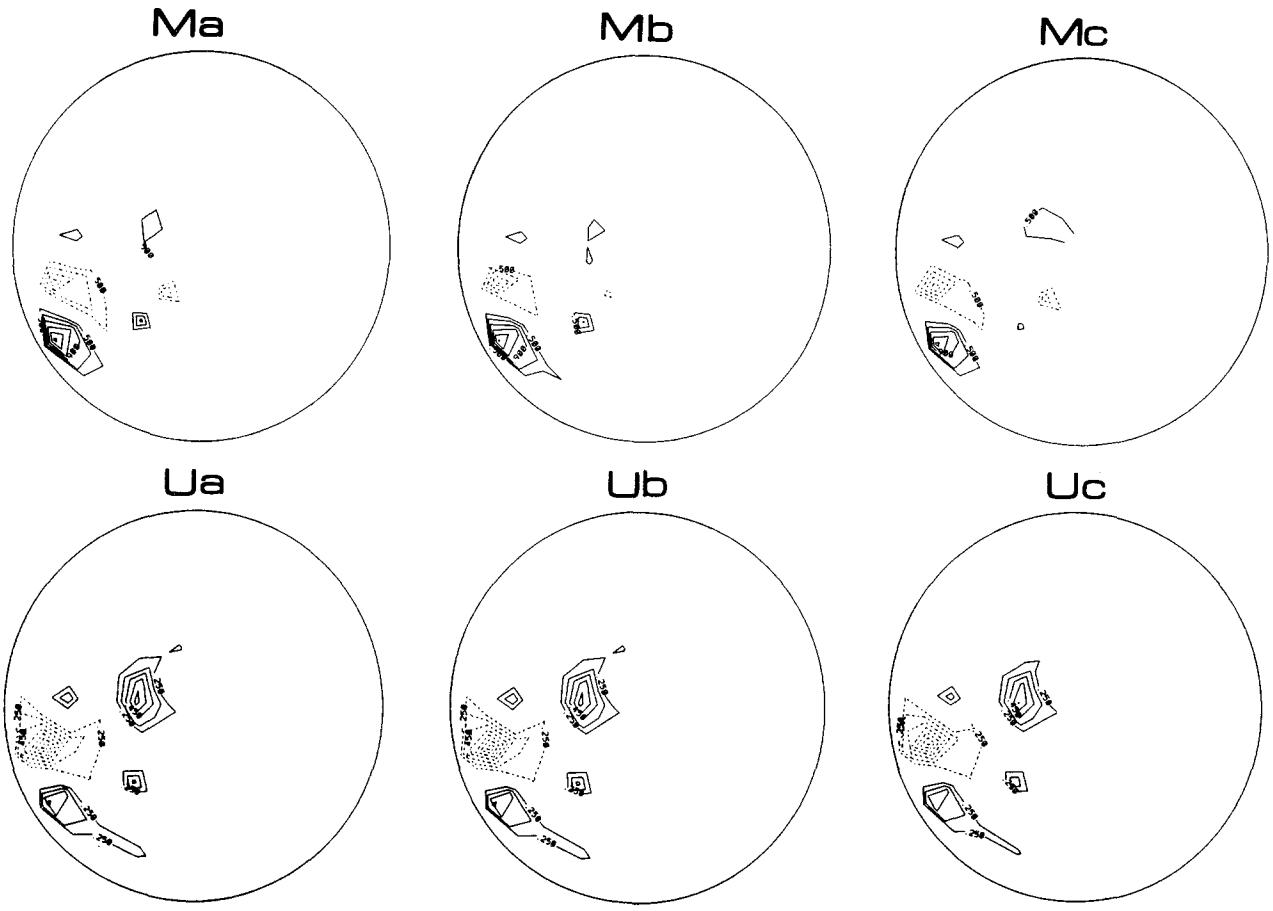

Figure 13. Median (upper row) and ulnar (lower row) somatosensory evoked Laplacian at a latency of 24 ms. Each plot was obtained as an average of the responses of 500-700 stimuli. The maximum prestimulus level ("background Laplacian") was removed. The three columns represent three separate trials for each nerve. Laplacian plots are consistently reproducable if both subject and nerve are fixed. There is, however, significant inter subject variability (Law 1991).

laboratory was presented earlier (Pilgreen et al. 1989; Nunez 1989b). The experimental protocol for head digitization, calculation of Laplacian maps, and NCAR plotting is nearly identical to that of the somatosensory evoked potential studies. However, in the P300 studies, 31 electrodes were placed over the entire head (4.6 cm average spacing). A right ear reference was chosen, and the left ear was recorded with respect to the right in order to transform potentials to a "mathematically linked ears" record. Although Laplacian maps are expected to be independent of reference, we have chosen this procedure in order to match standard methods.

High and low pass filters on the Pathfinder were set at 0.5/30 Hz; a 60 Hz notch filter was applied. The sampling rate was 256 Hz/channel. Rare (20%, 1500 Hz, 90dBHL) and frequent tones (80%, 750 Hz, 90dBHL) were presented randomly to both ears on a white noise background (65dBHL). Single, 1-sec epochs were collected (200 ms pre-stimulus, 800 ms post-stimulus) and viewed by an experienced neurophysiologist (KLP) in order to reject obvious artifacts. The decision time used to either store or reject single epochs tended to randomize the interstimulus interval.

Each trial evoked potential consisted of an average of 10-13 epochs free of obvious artifacts. Three trials were obtained on subject GH. Surface potential and Laplacian maps for the three trials were very similar, the principal difference being a reduction in potential and Laplacian magnitudes of P300's obtained in later trials. The potential and Laplacian waveforms from trial two of the three trials are shown as a function of latency in figure 14. Both similarities and differences are observed when comparing potential to Laplacian time series. For example, the P3 Laplacian peak at 200 ms is in phase with the corresponding potential peak. However, the P4 Laplacian at 200 ms is out of phase with both P3 potential and

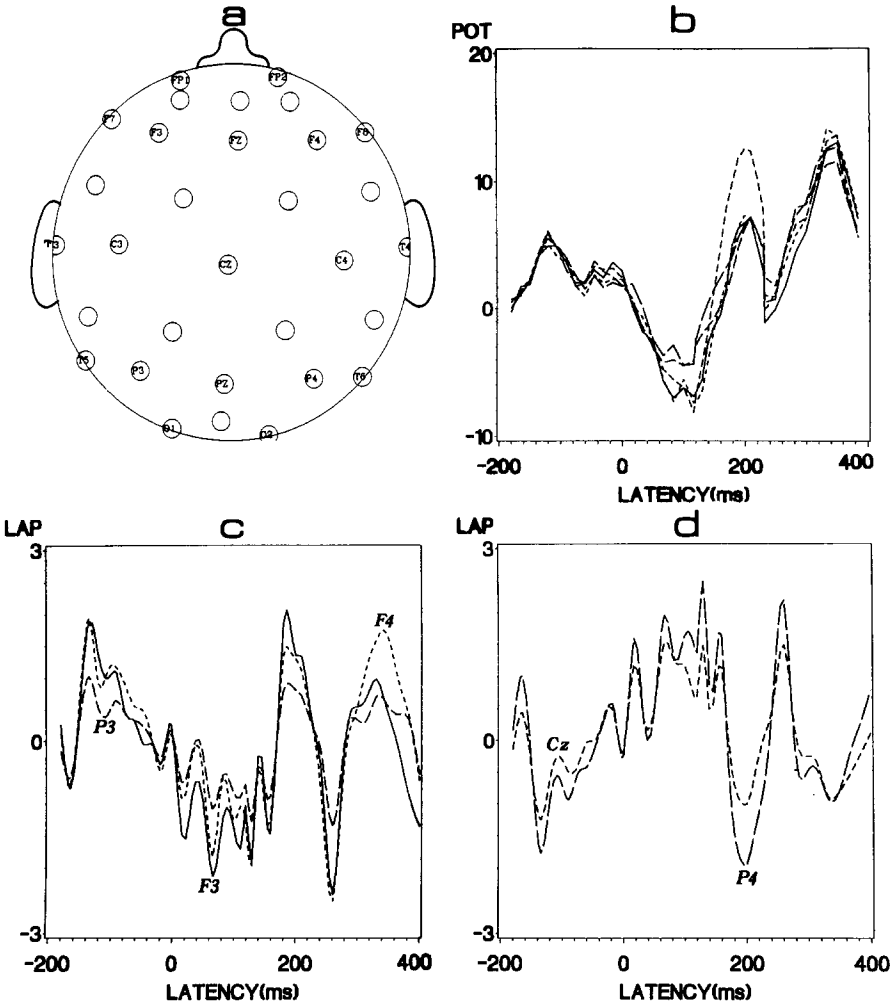

Figure 14. Potential (upper right) and Laplacian (lower row) time series (5 of 31 data channels) for auditory stimulation (Laplacian shown in two plots for clarity). Trial 2 (of 3 trials) for subject GH. Waveforms based on an average of 12 epochs of rare tone stimulation (100 total stimuli, some "rare epochs" rejected because of artifact).

Laplacian. Note, however, that the potential waveforms are reference dependent, e.g., a positive potential at some fixed latency might be negative with a different choice of reference. This occurs because "potential", by itself, has no direct physical meaning; it is only the *difference* or *gradient* of potential that has meaning. By contrast, the Laplacian is an estimate of a real physical quantity, i.e., the current flowing through the skull into the scalp (Nunez 1981). There is no ambiguity about either its magnitude or its sign; the main issue is that of the accuracy of the estimate.

The surface Laplacian at major peaks of the auditory evoked potential is shown in figure 15. These maps suggest specific clumps of cortical sources. The most dominant coherent sources of P300 appear to occur in prefrontal cortex, a result obtained in all trials of all four subjects studied thus far. Of course, this result tells us nothing about the possible involvement of subcortical structures since the Laplacian is insensitive to more distant sources. Also, the marginal sampling obtained with only 31 electrodes over the whole head provides a spatial resolution that is substantially inferior to many of our mathematical simulations and to the somatosensory evoked Laplacians shown here. Thus, we are unable to categorize apparent P300 sources beyond noting the apparent frontal dominance of coherent sources. In plotting figure 15, we have subtracted the *average* RMS, pre-stimulus Laplacian rather than the maximum pre-stimulus Laplacian (as was the procedure for the SEP plots). This choice was motivated by our uncertainty as to the significance of pre-stimulus sources that might occur due to anticipation of the stimulus. If we subtract the *maximum* pre-stimulus Laplacian, *all* P300 "sources" occur in prefrontal cortex.

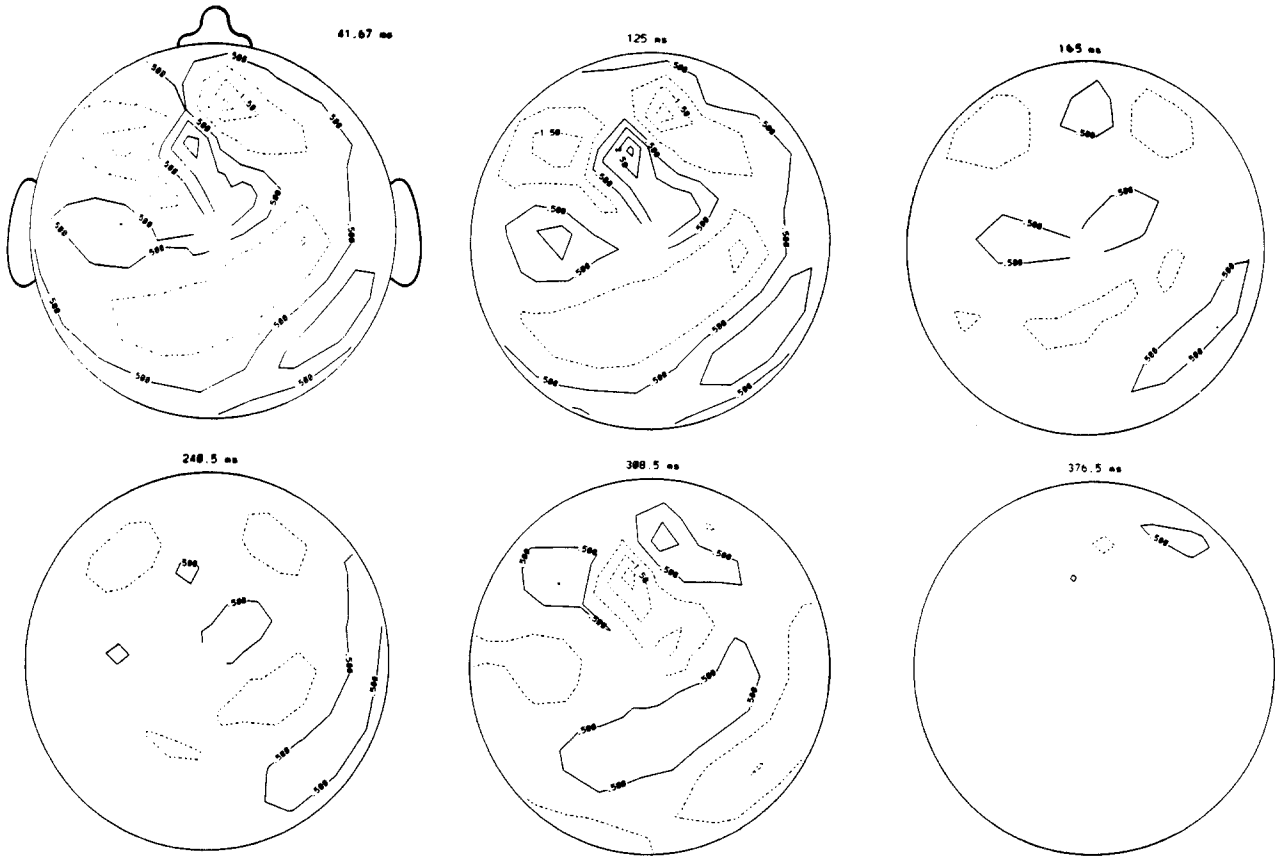

Figure 15. NCAR Laplacians of the auditory evoked potential shown in figure 14. Each plot corresponds to the latency (ms) shown. The average rms pre-stimulus Laplacian has been subtracted from each map. Contours are labeled in mV/cm2.

The Future of High Resolution EEG

Various surface Laplacians have now been tested using hundreds of mathematical simulations (Nunez 1981, 1989c, 1990b; Katznelson 1981; Perrin et al. 1987a, 1989; Law 1991), spontaneous EEG (Hjorth 1975; Nunez 1981; Katznelson 1981; Nunez and Pilgreen 1991), evoked potentials (Gevins and Cutillo 1986; Gevins 1987; Perrin et al. 1987b; Giard et al. 1988; Nunez 1988, 1989c, 1990a,b; Nunez and Pilgreen 1991; ; Nunez et al. 1991; Law 1991), and epileptic spikes (Pilgreen and Nunez 1989; Nunez and Pilgreen 1991; Nunez 1989c, 1990b). The extension of the original Laplacian approach (Hjorth 1975) to the more accurate spline-based Laplacians by the French group (Perrin et al. 1987a,b) has proven to be a highly siginificant step; for comparisons of the various Laplacians, refer to (Nunez 1990b; Law 1991; Nunez and Pilgreen 1991). These studies suggest that new, high resolution EEG systems, based at least partly on surface Laplacian methods, should soon become widely available. Once implemented, the surface Laplacian is likely to remain an important tool in EEG for some time, even if model-dependent approaches (e.g., dipole localization and spatial deconvolution) come into common practice. This claim for the Laplacian is made because of its applicability to distributed cortical sources and its insensitivity to head model errors.

Specific developments of spline Laplacian methods either completed or planned for the near future by the Brain Physics Group at Tulane University include:

1. Simplification of the experimental protocol and data analysis. For example, we now used four separate computer systems. This has been partly accidental, but mostly due to the fact that certain software packages (e.g., IMSL, SAS, NCAR) are readily available (e.g., without excessive cost) only on some computers. One solution is to develop our own software and carry out all analyses on a dedicated workstation, with hardware cost in the 10K range.

2. Increase the density of electrodes. Dramatic improvements in spatial resolution with the Laplacian are only possible when applied to data obtained with closely

spaced electrodes. If the whole head is to be surveyed, at least 31 channels should probably be used, since the spatial scale at which detail is observed can never be smaller than the distance between electrodes. Ideally, one would like to have a maximum electrode spacing of 2 cm (roughly 128 channels for full head sampling), and there is reason to expect some improvement in accuracy with even denser arrays. Of course, there are many kinds of studies in which data can be recorded over only parts of the head, or in serial recordings using the whole head. Furthermore, spatial resolution in studies involving gross comparisons of large regions (e.g., cerebral lateralization) can be dramatically improved with only ten EEG channels used to compute Hjorth Laplacians (Nunez et al. 1985; Nunez and Pilgreen 1991).

3. Improvement of the surface Laplacian algorithm. One of us has developed the surface Laplacian for the best fit ellipsoid (Law 1991). This work was motivated by an earlier study showing that upper surfaces of human heads can be fitted to general ellipsoids (i.e., by finding the center and three axes) with a typical accuracy in the 0.5 cm range (Law and Nunez 1991). Some further testing is required before routine implementation of the ellipsoid surface Laplacian, however. Also, graphics programs must be developed for mapping Laplacians on ellipsoidal surfaces, thereby replacing the NCAR plots.

4. Coordination of surface Laplacian estimates with MRI data. This will be especially interesting when the surface Laplacian algorithm based on ellipsoidal surfaces is implemented.

5. Correction of the surface Laplacian map due to local skull resistance variations. This will require new methods to estimate the skull resistivity function (Nunez 1987b) as well as geometric information from MRI.

6. The development of pattern recognition algorithms, using improved spatial resolution obtained with the spline-Laplacian, to study brain dynamics (Nunez 1989a,c, 1991; Ingber and Nunez 1990). This will also require more efficient algorithms to speed up the calculation of spline-Laplacians at many successive time points of spontaneous EEG, or individual (unaveraged) evoked potentials as required to obtain high resolution estimates of correlation function coefficients. The latter approach to evoked potentials has long been followed by Gevins and coworkers, but with most published Laplacians based on a nearest-neighbor algorithm. Recently, this group has implemented a new 3-dimensional Laplacian (Gevins et al. 1990; Gevins et al. 1991).

References

Cohen, D., Cuffin, B.N., Yunokuchi, K., Maniewski, R., Purcell, C., Cosgrove, G.R., Ives, J. and Kennedy, J. MEG versus EEG localization test using implanted sources in the human brain. Ann. Neurology, 1990, 28: 811-817.

Cooper, R., Winter, A.L., Crow, H.J. and Walter, W.G. Comparison of subcortical, cortical and scalp activity using chronically indwelling electrodes in man. Electroencephal. Clin Neurophysiol., 1965, 18: 217-228.

Cuffin, B.N. Effects of fissures in the brain on electroencephalograms and magnetoencephalograms. J. Appl Physics, 1985, 57: 146-153.

Cuffin, B.N. and Cohen, D. Comparison of the magnetoencephalogram and electroencephalogram. Electroencephal. Clin. Neurophysiol., 1979, 47: 132-146.

Cuffin, B.N., Cohen, D., Yunokuchi, K., Maniewski K.R., Purcell C., Cosgrove, G.R., Ives, J., Kennedy, J. and Schomer, D. Tests of EEG localization accuracy using implanted sources in the human brain. Ann. Neurology, 1991, 29: 132-138.

DeLucchi, M.R., Garoutte, B. and Aird, R.B. The scalp as an electroencephalographic averager. Electroenceph. Clin Neurophysiol., 1975, 38: 93-96.

Desmedt, J.E. and Tomberg, C. Topographic analysis in brain mapping can be compromised by the average reference. Brain Topography, 1990, 3: 35-42.

Desmedt, J.E., Chalkin, V., and Tomberg, C. Emulation of SEP components with the 3-shell model and the problem of "ghost potential fields" when using an average reference in brain mapping. Electroenceph. Clin. Neurophysiol., 1990, 77: 243-258.

Fender, D.H. Source localization of brain electrical activity. In: Gevins, A.S. and Remond, A. (Eds), Handbook of Electroencephalography and Clinical Neurophysiology, Revised Series, vol. 1, Elsevier Press, New York, 1987, 355-403.

Freeman, W. Use of spatial deconvolution to compensate for distortion of EEG by volume conduction. IEEE Trans. Biomed Eng., 1980, 27: 431-429.

Gevins, A.S. Obstacles to Progress, In: Gevins, A.S. and Remond, A. (Eds), Handbook of Electroencephalography and Clinical Neurophysiology, Revised Series, Vol. 1, New York, Elsevier Press, 1987, 665-673.

Gevins, A.S. Analysis of multiple lead data. In: Rohrbaugh, J.W, Parasuraman, R. and Johnson, J.R. (Eds), Event-Related Brain Potentials, Oxford University Press, New York, 1990, 44-56.

Gevins, A.S. and Cutillo B.A. Signals of congition. In: Lopes da Silva, FH (Ed), Handbook of Electroencephalography and Clinical Neurophysiology, Revised Series Vol. 2, Elsevier Press, New York, 1986, 335-381.

Gevins, A.S., Brickett, P., Costales, B., Le, J. and Reutter, B. Beyond topographic mapping: towards functional-anatomical imaging with 124-channel EEGs and 3-D MRIs. Brain Topography, 1990, 3: 53-64.

Gevins, A.S., Le, J., Brickett, P., Reutter, B., and Desmond, J. Seeing through the skull: Advanced EEG's accurately measure cortical activity from the scalp. Brain Topography, 1991, 4: 125-132.

Giard, M.H., Perrin, F., Pernier, J. and Peronnet, F. Several attention-related wave forms in auditory areas: a

topographic study. Electroenceph. Clin. Neurophysiol., 1988, 69: 371-384.

Hari, R. and Kaukoranta, E. Neuromagnetic study of somatosensory system: principles and examples. Prog. Neurobiol., 1985, 24: 233-256.

He, B., Busha, T., Okamoto, Y., Homma, S., Nakajima, Y. and Sato, T. Electric dipole tracing in the brain by means of the boundary element method and its accuracy. IEEE Trans. Biomed. Eng., 1987, 34: 406-413.

Henderson, C.J., Butler, S.R. and Glass, A. The localization of equivalent dipoles of EEG sources by the application of electric field theory. Electroenceph. Clin. Neurophysiol., 1975, 39: 117-130.

Hjorth, B. An on-line transformation of EEG scalp potentials into orthogonal source derivations. Electroenceph. Clin. Neurophysiol., 1975, 39: 526-530.

Ingber, L. and Nunez, P.L. Multiple scales of statistical physics of neocortex: application to electroencephalography. Mathl Comput. Modelling, 1990, 13: 83-95.

Katznelson, R.D. Chapter 6 in Nunez, P.L. Electric Fields of the Brain: The Neurophysics of EEG. Oxford University Press, New York, 1981.

Katznelson, R.D. Deterministic and Stochastic Field Theoretic Models in the Neurophysics of EEG. Ph.D. Dissertation, University of California at San Diego, La Jolla, 1982.

Kavanagh, R.N., Darcey, T.M., Lehmann, D. and Fender, D.H. Evaluation of methods for three-dimensional localization of electrical sources in the human brain. IEEE Trans. Biomed. Eng., 1978, 24: 421-429.

Kearfott, R.B., Sidman, R.D., Major, D.J. and Hill C.D. Numerical tests of a method for simulating electrical potentials on the cortical surface. IEEE Trans. Biomed. Eng., 1991, 38: 294-299.

Law, S.K. and Nunez, P.L. Quantitative representation of the upper surface of the human head. Brain Topography, 1991, 3: 365-371.

Law, S.K. Spline Generated Surface Laplacians for Improving Spatial Resolution in Electroencephalography. Ph.D Dissertation, Tulane University, New Orleans, 1991.

Lopes da Silva, F.H. and Storm van Leeuwen, W. The cortical alpha rhythm in dog:the depth and surface profile of phase. In: Brazier, MBA and Petsche, H (Eds.), Architectonics of the Cerebral Cortex, Raven Press, New York, 1978, 319-333.

Nicholas, P. and Deloche G. Convolution computer processing of the brain electrical image transmission. Int. J. Biomed. Comput., 1976, 7: 143-159.

Nunez, P.L. Electric Fields of the Brain: The Neurophysics of EEG. Oxford University Press, New York, 1981.

Nunez, P.L. The brain's magnetic field: some effects of multiple sources on localization methods. Electroenceph. Clin. Neurophysiol., 1986, 63: 75-82.

Nunez, P.L. A method to estimate local skull resistance in living subjects. IEEE Trans. Biomed. Eng., 1987a, 34: 902-904.

Nunez, P.L. Removal of reference electrode and volume conduction effects by spatial deconvolution of evoked potentials using a three-concentric sphere model of the head. The London Symposium. Electroenceph. Clin. Neurophysiol. [Suppl], 1987b, 39: 143-148.

Nunez, P.L. Spatial filtering and experimental strategies in EEG. In: Samson-Dollfus, D. (Ed), Statistics and Topography in Quantitative EEG. Elsevier, Paris, 1988, 196-209.

Nunez, P.L. Towards a physics of neocortex. In: Marmarelis, V.Z. (Ed), Advanced Methods of Physiological Systems Modeling. Plenum Press, New York, 1989a, 241-259.

Nunez, P.L. Estimation of large scale neocortical source activity with EEG surface Laplacians. Brain Topography, 1989b, 2: 141-154.

Nunez, P.L. Generation of human EEG by a combination of long and short range neocortical interactions. Brain Topography, 1989c, 1: 199-215.

Nunez, P.L. Physical principles and neurophysiological mechanisms underlying event related potentials. In: Rohrbaugh, J., Johnson, R., Parasuraman, R. (Eds), Event Related Potentials of the Brain. Oxford University Press, New York, 1990a, 19-36.

Nunez, P.L. Localization of brain activity with electroencephalography. In: Sato, S. (Ed), Advances in Neurology, vol 54, Magnetoencephalography. Raven Press, New York, 1990b, 39-65.

Nunez, P.L. Neocortical dynamics at the macroscopic scale of electroencephalography: physical analogs. Proc. Eighth Inter. Conf. Mathl. Comput. Modelling, College Park, Maryland, April, 1991.

Nunez, P.L., Javorski, L. and Nelson, A.V. Unpublished pilot study of Brain Physics Group, Tulane University, 1985.

Nunez, P.L. and Pilgreen, K.L. Laplacian evaluation of epileptic spike foci. American Electroencephalographic Society Annual Scientific Meeting, San Diego, October 2-5, 1988.

Nunez, P.L. and Pilgreen K.L. The spline Laplacian in clinical neurophysiology: a method to improve EEG spatial resolution. J. Clin. Neurophysiol., 1991, in press.

Nunez, P.L., Pilgreen, K.L. and Law, S.K. Mapping of evoked potentials. In: Barber, C. and Taylor, M.J. (Ed), Evoked Potentials Review. Elsevier Press, New York, 1991, 57-64.

Perrin, F., Bertrand, O. and Pernier, J. Scalp current density mapping: value and estimation from potential data. IEEE Trans. Biomed. Eng., 1987a, 34: 283-288.

Perrin, F., Pernier, J., Bertrand, O., Giard, M.H. and Enchallier, J.F. Mapping of scalp potentials by surface spline interpolation. Electoenceph. Clin. Neurophysiol., 1987b, 66: 75-81.

Perrin, F., Pernier, J., Bertrand, O., and Echallier, J.F. Spherical splines for scalp potential and current density mapping. Electroenceph. Clin. Neurophysiol., 1989, 72: 184-187.

Petsche, H., Pockberger, H. and Rappelsberger, P. On the search for the sources of the electroencephalogram. Neuroscience, 1984, 11: 1-27.

Pilgreen, K.L. and Nunez, P.L. Source variability of interictal spike foci, The Southern EEG Society and Southern Society of EEG Technologists Joint Meeting, St. Petersburg, January 12-14, 1989.

Regan, D. Human Brain Electrophysiology. Evoked Potentials and Evoked Magnetic Fields in Science and Medicine. Elsevier Press, New York, 1989.

Romani, G.L. and Rossini, P. Neuomagnetic functional localization: principles, state of the art, and perspectives. Brain Topography, 1988, 1: 5-21.

Rush, S. and Driscoll, D.A. Current distribution in the brain from surface electrodes. Anesth. Analg., 1968, 47: 717-723.

Rush, S. and Driscoll, D.A. EEG electrode sensitivity: an application of reciprocity. IEEE Trans. Biomed. Eng., 1969, 16: 15-22.

Scherg, M. Fundamentals of dipole source potential analysis. In: Hoke, M., Grandori, F. and Romani, G.L. (Eds), Auditory evoked magnetic fields and potentials. Advances in Neurology, vol 6. Basel:Karger, 1989.

Scherg, M. and von Cramon, D. Two bilateral sources of the late AEP as identified by a spatio-temporal dipole model. Electroenceph. Clin. Neurophysiol., 1985, 62: 32-44.

Scherg, M. and von Cramon, D. Dipole source potentials of the auditory cortex in normal subjects and in patients with temporal lobe lesions. In:Hoke, M., Grandori, F. and Romani, G.L. (Eds.), Auditory evoked magnetic fields and potentials. Advances in Audiology, vol 6. Basel:Karger, 1989.

Sepulveda, N. Electric Field Distribution in Three Dimensional Regions Using the Finite Element Method. Ph.D. Dissertation, Tulane University, New Orleans, Louisiana, 1984.

Weinberg, H., Brickett, P., Robertson, A., Harrop, R., Cheyne, D.O., Crisp, D., Baff, M. and Dykstra, C. The location of source-systems in the brain: early and late components of event-related potentials. J. Alcoholism, 1987, 4: 339-345.

Williamson, S.J. and Kaufman, L. Analysis of neuromagnetic signals. In:Gevins, A.S. and Remond, A. (Eds), Handbook Of Electroencephalography And Clinical Neurophysiology, Revised Series, Volume 1, Elsevier Press, Amsterdam, 1987, 405-488.

Wood, C.C. Application of dipole localization methods to source identification of human evoked potentials. Annals of the New York Academy of Sciences, 388: 139-155.

Yan, Y., Nunez, P.L. and Hart, R.T. A finite element model of the human head: scalp potentials due to dipole sources. Medical and Biological Engineering and Computing, Sept., 1991, in press.